Experimental evaluation of cMUT and PZT transducers in receive only mode for photoacoustic imaging

O. Warshavski [a], C. Meynier* [a], N. Sénégond [a], P. Chatain [a],
Johannes Rebling [b,c], Daniel Razansky [b,c], N. Felix [a], A. Nguyen-Dinh [a];
[a] Advance Research Department, VERMON 180 Rue du General Renault 37038 Tours, France
[b] Institute for Biological and Medical Imaging (IBMI), Helmholtz Zentrum München, Germany, Ingoldstädter Landstraße 1, 85764 Neuherberg, Germany
[c] School of Medicine and School of Electrical Engineering and Information Technology, Technische Universität München, München, Germany

ABSTRACT

The angular reception performance of ultrasound transducers is a critical parameter in the design of a photoacoustic imaging system. Here we present a quantitative comparison between cMUT and PZT ultrasound transducers. We analyze the requirements of an ideal transducer for conventional pulse-echo ultrasound versus those of a photoacoustic imaging transducer. We show the significant benefits of cMUT based transducers over conventional PZT arrays. This strongly suggest that cMUT transducer can be used to greatly improve the image quality and sensitivity of photoacoustic systems.

Keywords: cMUT, PZT, Photoacoustics, Optoacoustic, OA Imaging, PA Imaging, Transducers, Array, NEP

1. INTRODUCTION:

Photoacoustic (PA, also call optoacoustic) imaging offers clinical applications due to its capability to overcome the scattering barrier that limits other light-based imaging modalities to penetration depths of approximately one millimeter in biological tissue[1]. Nowadays, state of the art ultrasound (US) imaging offers real time, three dimensional, multiscale images with a high depth penetration and with good spatial resolution. In addition, US enables the visualization of vascular flows and mechanical properties using elastography[2, 17]. Photoacoustic imaging on the other hand can benefit physicians mainly due to its unique ability to differentiate tissue characteristics with high specificity, using several wavelengths and provide delineate vascularization[3], with clear identification of oxygenation and hemoglobin content[4]. Most demonstrations of PA imaging and Photoacoustic Tomography (PAT) currently use commercially available, conventional US transducers based on piezoelectric materials such as PZT or PZT-based composites. Recently, several publications have assessed the feasibility of using capacitive micromachined ultrasound transducers (cMUT) for PA imaging[5-7], demonstrating experimentally significant enhancement of imaging quality characteristics such as contrast and SNR compared to PZT based transducers[8,9]. cMUT are manufactured using well established photolithography micromachining techniques which enables a flexible multiscale design, repetitive production and can be naturally integrated with other semiconductors technologies for maximized integration. The cMUT transducers used in those early studies were designed for pulse-echo US imaging. However, a distinction must be made between conventional ultrasound mode imaging (B-mode, Color Flow, CEUS, Elastography …) and PA imaging because they require significantly different transducer performances. We hereby demonstrate that transducer specifications should be customized to optimize the performance in PAI. Table 1 lists typical requirements between ultrasound and photoacoustics transducers, thus differences are being translated into the transducer design and are governing the performances which largely determine the image quality.

* Corresponding author: c.meynier@vermon.com

Photons Plus Ultrasound: Imaging and Sensing 2016, edited by Alexander A. Oraevsky, Lihong V. Wang
Proc. of SPIE Vol. 9708, 970830 · © 2016 SPIE · CCC code: 1605-7422/16/$18 · doi: 10.1117/12.2211799

Table 1 - Typical requirements from transducers for ultrasound and photoacoustics imaging

	Ultrasound	Photoacoustics
Bandwidth	80-100 %	>120%
Dynamic Range	100 kPa – 100 Pa	10 kPa - Pa
Functionality	transmit and receive	receive only
Sensitivity \ SNR \ NEP	relative (pulse echo)	absolute
Imaging Repetition Speed	Very high (limited by imaging depth)	Moderate (limited by laser system)
Directivity	Application depended	Low \ Uniform

To optimize a transducer technology, a clear definition of quantifiable characteristics is required. This enables a reliable comparison between different transducers and transducer technologies. For ultrasound it is common practice to use the pulse-echo measurement of a highly reflective target, as shown in (Fig. 2). The reflected US signals provide a good characteristic of the transducer performance in the time and frequency domain. Photoacoustic transducer characterization differs due to the lower amplitude, wide bandwidth and the omni-directionality of the photoacoustic signals. In this work we present three different quantifiable parameters that can be used to compare the performances of cMUT and piezoelectric based transducer (or any other type of transducer technology).

2. SETUP

A schematic overview of the measurement setup is shown in Fig. 1. The transmit element is an unfocused, 19mm diameter, PVDF broadband transducer (Precision Acoustics, PA801) excited by a commercially available pulse/receiver (5073PR, Olympus, Massachusetts, USA). Three axis and rotational positioning control is performed using an in-house made mechanical system controlled via MATLAB (MathWorks, U.S.A.).

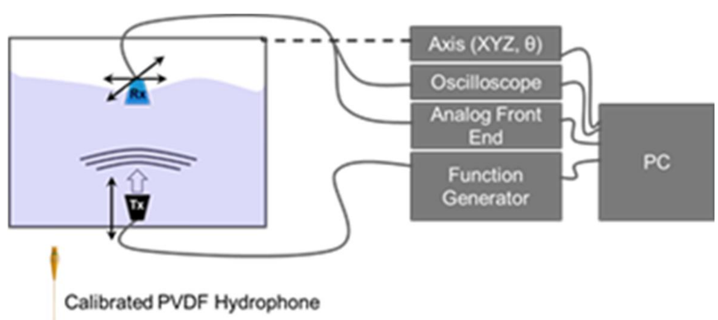

Figure 1 - Receive sensitivity measurement setup

The signal received by the transducer under test is recorded using a fully integrated US analog front end (AFE) evaluation board (Texas Instruments, AFE5809evm). The AFE's analog signal chain is comprised of low noise amplifiers (24 dB and 30 dB, total of 54 dB Gain), high pass (50 kHz) and antialiasing (15 MHz) filters and a 62.5 MHz analog to digital convertor with a resolution of 14 bits. The transmitted signal levels are calibrated using a needle hydrophone (Precision Acoustics, 0.2mm) which allows the precise measurement of the excitation pressure at the surface of the transducer under test. The alignment and measurement is performed using a MATLAB script.

3. RESULTS

The comparison of PZT versus cMUT transducers was performed using two linear array US transducers designed for superficial ultrasound imaging applications (Breast, Thyroid, and Superficial vascular). The two transducers have an inter-element pitch of 200µm, a transverse height of 8mm and 4mm, respectively, a comparable broadband response (cMUT 116%, PZT 82%) and similar center frequencies (cMUT 5MHz, PZT 7MHz) [10]. The conventional pulse-echo time and frequency responses of both the cMUT (a) and PZT (b) transducers are show in Figure 2.

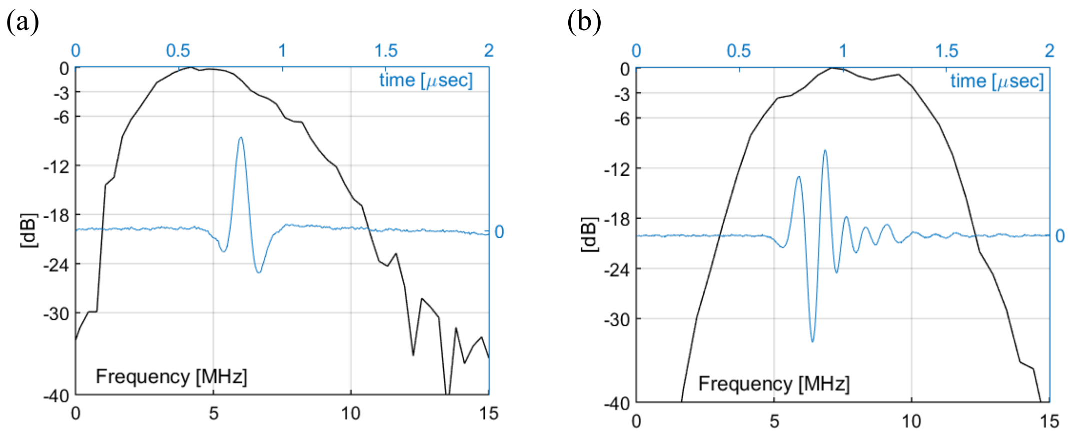

Figure 2 - Conventional pulse-echo characterization of (a) cMUT and (b) PZT transducer elements.

The angular directivity pattern (between -80° and 80°) from a broadband pulse excitation, which enables to obtain accurate measurement using a single angular mechanical scan. The scale of the frequency responses is determined by normalizing the spectrums with the peak value. Fig. 3(a) and (b) present equal-sensitivity contours over the Frequency-Incident angle domain for a broadband (short pulse) excitation of a cMUT (PZT) transducer single element, biased at 85V (80% collapse voltage), for angles between -80° and 80°. The Fig. 3(c) and (d) present the frequency response at specific angles (0°, ±20°, ±40° and ±60°) for a cMUT (PZT) transducer. Fig 3(e) and (f) presents the receive directivity at specific frequencies (2.0MHz, 5.0MHz, 7.0MHz and 10.0MHz).

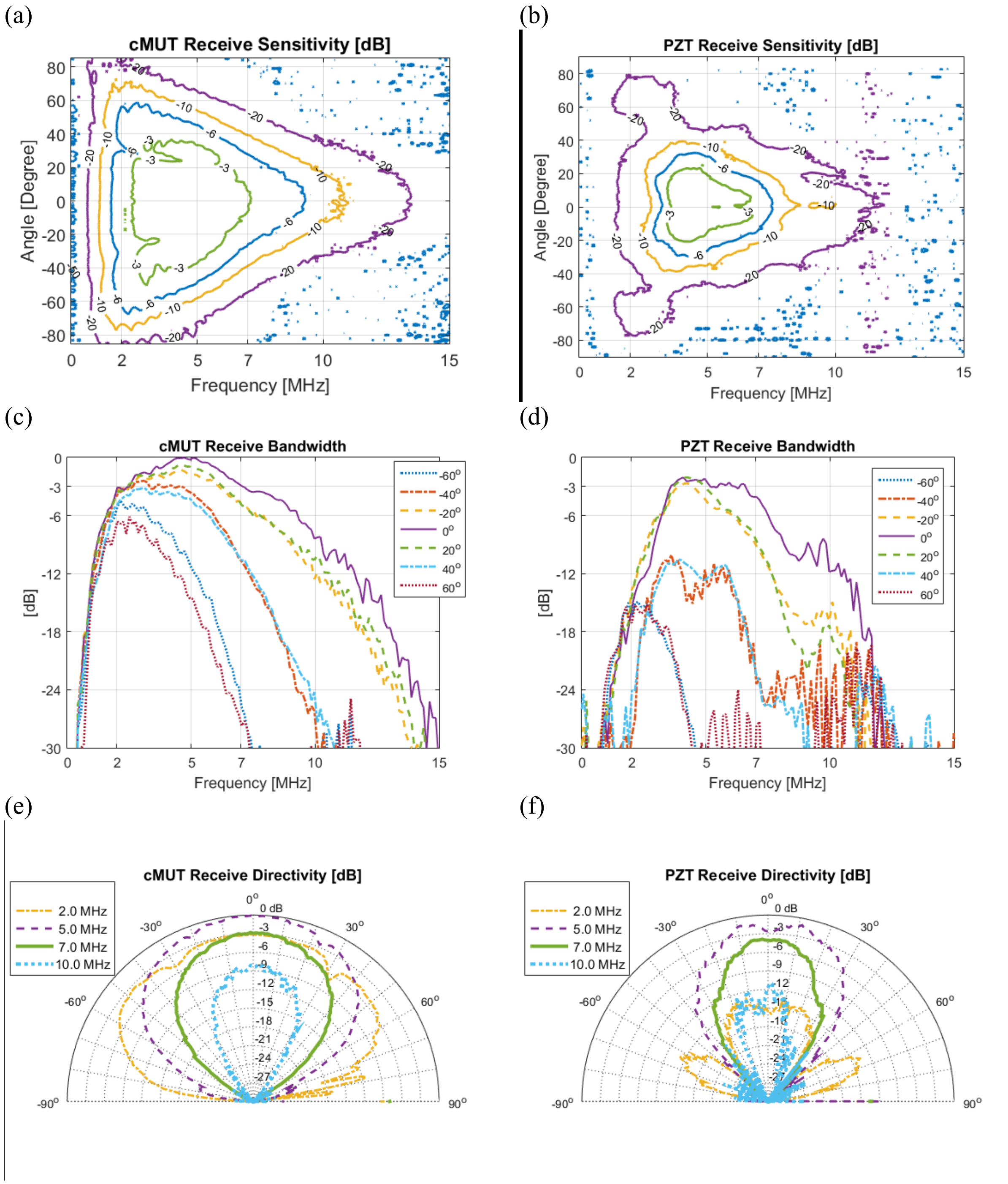

Figure 3 - Angular sensitivity measurement by a broadband pulse excitation. All measurement performed using a single element of the transducer arrays with cMUT (a), (c) and (e) in the left column and PZT (b), (d) and (f) in the right column. (a) and (b) Equal-sensitivity contours as a function of frequency and incident angle. (c) and (d) Frequency response at specific angles (0°, ±20°, ±40° and ±60°). (e) and (f) Receive directivity at specific frequencies (2.0 MHz, 5.0 MHz, 7.0 MHz and 10.0 MHz).

4. DISCUSSION

The experimental comparison of the cMUT and PZT transducer demonstrates the high sensitivities of cMUT and PZT over wide range of frequencies and confirms the broadband response for both technologies within the one to ten megahertz range as is indicated by the large fractional bandwidth in table 2. The cMUT element has a favorable fractional bandwidth over the whole angle range. The cMUT low cutoff frequency is considerably lower than that of the PZT as is also indicated by the pulse echo characterization shown in Fig 2. In contrast to the high cutoff frequency of the PZT in the pulse echo characterization, the high cutoff of the cMUT is almost consistently higher than that of the PZT in the Receive only characterization. This is due to the fact that the transmitted and received responses of the PZT based transducer are almost identical whereas for cMUT, the transmit transfer and receive transfer functions are different, due to the nonlinearity of the transfer function[11].

Table 2 - Low and High cutoff frequency and fractional bandwidth for cMUT and PZT elements at different angles

		cMUT			PZT		
		Low Cutoff [MHz]	High Cutoff [MHz]	Fractional Bandwidth	Low Cutoff [MHz]	High Cutoff [MHz]	Fractional Bandwidth
0°	3dB	2.0	7.2	113%	3.2	7.2	77%
	6dB	1.5	9.3	144%	2.9	8.2	95%
±20°	3dB	1.9	6.7	112%	3.3	5.6	52%
	6dB	1.4	8.4	143%	2.6	7.0	92%
±40°	3dB	1.6	5.8	114%	2.9	6.2	73%
	6dB	1.3	6.6	134%	2.7	6.5	83%
±60°	3dB	1.5	4.5	100%	1.6	3.2	67%
	6dB	1.1	4.7	124%	1.1	3.8	110%

As can be observed from fig. 3(a) and (b), the frequency dependence of the angular frequency response is becoming dominant when half of the acoustical wavelength is approaching the element pitch size of 200µm (3.75 MHz). This effect is more pronounced in the case of the cMUT since it has a lower cutoff frequency compared to the PZT. The frequency dependence of the acceptance angle emphasizes the importance of detailed matching between the geometrical layout of transducer elements and the detailed characterization of the transducer for specific application due to the complex acoustic dependencies that come to play during the transducer design process.

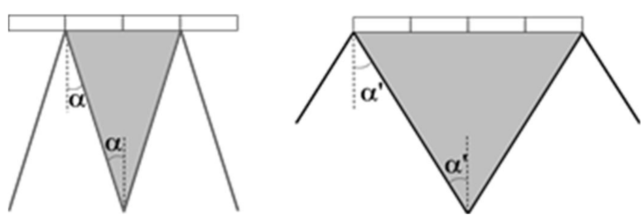

Figure 4- Geometrical equivalency between the acceptance angle and the f-number

Fig. 4 shows the geometrical equivalency between the acceptance angle and the f-number of an array. A smaller f-number (large acceptance angle) affects the received signal and hence the image quality both by increasing the effective area of the transducer (improving the SNR) and by recording higher spatial frequency (improving the image resolution). The effects of the f-number on the image quality is stronger in PA imaging due to the omnidirectional propagation of acoustic waves.

*Table 3 - Acceptance angle and numerical aperture for cMUT and PZT elements at different frequencies, * main lobe.*

		cMUT		PZT	
		acceptance angle	f-number	acceptance angle	f-number
2.0 MHz	3dB	± 62°	1.1	± 31° *	1.9
	6dB	± 69°	1.1	± 36° *	1.7
5.0 MHz	3dB	± 35°	1.7	± 23°	2.6
	6dB	± 48°	1.3	±31°	1.9
7.0 MHz	3dB	± 27°	2.2	± 18°	3.2
	6dB	± 38°	1.6	± 24°	2.5
10.0 MHz	3dB	± 12°	4.8	± 10°	5.8
	6dB	± 26°	2.3	± 16°	3.6

The favorable f-number of cMUT over PZT which is clearly shown in fig. 3 and table 3, explains the favorable SNR and CNR of cMUT over PZT transducers previously demonstrated [8, 9].

The main drawback of the broadband excitation characterization results from its limited ability to compare between the calibrated transducer sensitivities ($mV/kPa/mm^2$) when the PZT transducer show typically about 12dB higher sensitivities in the central frequency for plane wave incident normal to the element plane compared with cMUT [12].

5. CONCLUSIONS

We present a side-by-side comparison of the sensitivity as a function of incident angle and frequency for both cMUT and PZT transducer elements. The quantitative characterization serves as a basis for a performance analysis between similar transducer designs, which is a critical step for further performance optimization in PA and US imaging systems at both transducer and system levels. The presented measurements can be taken as a reference for typical scale for the performances of cMUT and PZT technologies. Nevertheless, the performances of both transducer technologies result from balancing between multiple designs parameters and considerations.

The inherent characteristics (high bandwidth and low directivity) of cMUT transducers as well as their flexible geometrical design layout make them a highly suitable technology for PA imaging applications. Advanced designs of cMUT can improve their sensitivities [13]. Taking into consideration that PA optimized transducers might require only reception capabilities, changing the transducer design constraints and ease tight integration with low noise amplifiers. Such integration can potentially reduce parasitic\external noises and dramatically decrease the noise equivalent pressure below the limit of 1 Pascal, while maintaining high bandwidth, high acceptance angle and high sensitivity [14-16]. Thus a system level design that will include integration and design optimization of cMUT for receive only mode can significantly improve detection capabilities as compared to the current state-of-the-art transducers technology. The transducer specifications should be customized to optimize the performance in PAI, thus differences are being translated into the transducer design and are governing the performances which largely determine the image quality.

6. ACKNOWLEDGMENTS

This work has been supported by the European Union OILTEBIA (Optical Imaging and Laser Techniques for Biomedical Applications) Grant Agreement Number 317526.

7. REFERENCES

[1] Ntziachristos, V. “Going deeper than microscopy: the optical imaging frontier in biology”. Nature methods, 7(8), 603-614., (2010).

[2] Macé, E., Montaldo, G., Cohen, I., Baulac, M., Fink, M., & Tanter, M., “Functional ultrasound imaging of the brain”. Nature methods, 8(8), 662-664. (2011).

[3] Zhang, E. Z., Laufer, J. G., Pedley, R. B., & Beard, P. C., “In vivo high-resolution 3D photoacoustic imaging of superficial vascular anatomy”, Phys. Med. Biol. 54, 1035–1046 (2009).

[4] Dean-Ben, X. L., Razansky, D., “Adding fifth dimension to optoacoustic imaging: volumetric time-resolved spectrally enriched tomography”, Light: Science & Applications 3, (2014).
[5] Vaithilingam. S., Ma. T. J., Yukio Furukawa. Y., Oralkan. O., Kamaya. A., Torashima. K., Kupnik. M., Wygant. I. O., Zhuang. X., Jeffrey Jr. R. B. & Khuri-Yakub. B. T., “Investigating Large 2D Arrays for Photoacoustic and Acoustic Imaging using CMUT Technology”, IEEE International Ultrasonics Symposium Proc. (2010)
[6] Nikoozadeh. A., Choe. J. W., Kothapalli. S. R., Moini. A., Sanjani. S. S., Kamaya. A., Oralkan. O., Gambhir. S. S. & Khuri-Yakub. P. T., “Photoacoustic Imaging Using a 9F MicroLinear CMUT ICE Catheter” ”, IEEE International Ultrasonics Symposium Proc. (2012).
[7] Cheng. X., Chen. J. & Li. C., "A Miniature Capacitive Micromachined Ultrasonic Transducer Array for Minimally Invasive Photoacoustic Imaging", Systems, Journal of, (2010).
[8] Vallet, M., Varray, F., Kalkhoran, M. A., Vray, D., & Boutet, J. “Enhancement of photoacoustic imaging quality by using CMUT technology: Experimental study”. Ultrasonics Symposium (IUS), 2014 IEEE International (pp. 1296-1299). IEEE (2014).
[9] Legros, M., C. Meynier, R. Dufait, G. Ferin, & F. Tranquart. "Piezocomposite and CMUT arrays assessment through in vitro imaging performances." In Ultrasonics Symposium, 2008. IUS 2008. IEEE, pp. 1142-1145. IEEE, (2008).
[10] Clade. O., Felix. N., & Lacaze. E. “Linear and curved array with advanced electroacoustic and acoustic properties”, In Ultrasonics Symposium, 2002. Proceedings. Vol. 2, 1127-1130. IEEE (2002).
[11] Sénégond, N., Teston. F., D. Royer, Cyril Meynier, and Dominique Certon. "High voltage time domain response of cMUT membrane: Laser interferometry measurements." Physics Procedia 3, no. 1, 1011-1016 (2010).
[12] Oralkan. O., Jin. X., Degertekin. F. L. & Khuri-Yakub. B. T., "Simulation and experimental characterization of a 2-D capacitive micromachined ultrasonic transducer array element." Ultrasonics, Ferroelectrics, and Frequency Control, IEEE Transactions on 46, no. 6 1337-1340, (1999).
[13] Khuri-Yakub, B. T., & Oralkan, Ö. “Capacitive micromachined ultrasonic transducers for medical imaging and therapy”. Journal of micromechanics and microengineering, 21(5), 054004 (2011).
[14] Gurun, G., Hasler, P., & Degertekin, F. L. “Front-end receiver electronics for high-frequency monolithic CMUT-on-CMOS imaging arrays”. Ultrasonics, Ferroelectrics, and Frequency Control, IEEE Transactions on, 58(8), 1658-1668 (2011).
[15] Lemmerhirt, D. F., Cheng, X., White, R. D., Rich, C., Zhang, M., Fowlkes, J. B., & Kripfgans, O. D. “A 32 x 32 capacitive micromachined ultrasonic transducer array manufactured in standard CMOS”. Ultrasonics, Ferroelectrics, and Frequency Control, IEEE Transactions on, 59(7), 1521-1536. (2012).
[16] Wygant, I. O., Jamal, N. S., Lee, H. J., Nikoozadeh, A., Oralkan, O., Karaman, M., & Khuri-Yakub, B. T. “An integrated circuit with transmit beamforming flip-chip bonded to a 2-D CMUT array for 3-D ultrasound imaging”. Ultrasonics, Ferroelectrics, and Frequency Control, IEEE Transactions on, 56(10), 2145-2156. (2009).
[17] Errico, C., Pierre, J., Pezet, S., Desailly, Y., Lenkei, Z., Couture, O. and Tanter, M. "Ultrafast ultrasound localization microscopy for deep super-resolution vascular imaging." Nature 527, no. 7579 (2015): 499-502.